COMPDYN 2025
10th ECCOMAS Thematic Conference on
Computational Methods in Structural Dynamics and Earthquake Engineering
M. Papadrakakis, M. Fragiadakis (eds.)
Rhodes Island, Greece, 15-–18 June 2025

THE ROLE OF STORY LOSS FUNCTIONS IN REGIONAL SEISMIC VULNERABILITY MODELLING AND RISK ASSESSMENT

Davit Shahnazaryan[1,3], Volkan Ozsarac[1,3], and Gerard J. O'Reilly[2,3]

[1]Postdoctoral Researcher, Centre for Training and Research on Reduction of Seismic Risk (ROSE Centre)
Scuola Universitaria Superiore IUSS Pavia, Italy
{davit.shahnazaryan, volkan.ozsarac}@iusspavia.it

[2] Associate Professor, Centre for Training and Research on Reduction of Seismic Risk (ROSE Centre)
Scuola Universitaria Superiore IUSS Pavia, Italy
gerard.oreilly@iusspavia.it

[3] Djura — Risk - Data - Engineering, Pavia, Italy
{davit.shahnazaryan, volkan.ozsarac, gerard.oreilly}@djura.it

Keywords: storey loss function, seismic risk, vulnerability, loss, fragility.

Abstract. *Vulnerability functions quantify the relationship between seismic intensity and associated losses, playing a crucial role in regional seismic risk assessments and informing decision-making and risk-reduction strategies. A widely-used analytical approach to develop seismic vulnerability models for buildings is examined, integrating equivalent single-degree-of-freedom (SDOF) modelling, fragility functions, and damage-to-loss models. This paper is proposing an approach utilising story loss functions (SLFs) to more accurately calculate economic losses and their sources. The main advantage of this method lies in its ability to directly incorporate losses from floor accelerations and provide a detailed breakdown of losses across various building components. A case study comparison demonstrates the similarities between both methods and emphasises the enhanced benefits of using SLFs. This approach offers a more comprehensive framework for evaluating and communicating the contributions of structural, non-structural, and content losses across individual storeys of a building.*

1 INTRODUCTION

Assessing seismic risk is essential for understanding and reducing earthquake impacts on communities. By quantifying potential consequences of seismic events, we can identify vulnerable areas and prioritise risk reduction measures accordingly. Vulnerability functions are paramount in this assessment process, as they provide quantitative measurements of how structures might perform during earthquakes. These functions illustrate how damage-related losses may fluctuate depending on shaking intensity. Integrating vulnerability functions into risk assessment models enhances our understanding of potential earthquake impacts on buildings, infrastructure and populations. This integration enables prioritisation of retrofitting efforts and resource allocation, supports development of suitable emergency plans, and informs decisions on building regulations to strengthen resilience in earthquake-prone regions. Over recent decades, numerous methodologies for assessing seismic vulnerability have emerged, with Calvi et al. [1] offering a thorough examination of key developments. Particularly noteworthy was the shift towards analytical methodologies for quantifying structural seismic fragility. The displacement-based assessment methodology described by Calvi [2] and subsequently developed by Crowley et al. [3] and Borzi et al. [4] stands as a significant example. These approaches allow analysts to numerically model a building's expected mechanical behaviour and subsequently estimate its seismic vulnerability.

Further developments occurred during the late 2000s and early 2010s, with D'Ayala et al. [5] consolidating various approaches into comprehensive guidelines. A notable method within these guidelines involved using equivalent single-degree-of-freedom (SDOF) systems to represent entire building structures or classes when conducting larger regional seismic assessments. This approach offers exceptional computational efficiency with reasonable accuracy trade-offs. Silva et al. [6], provides additional considerations regarding this and other approaches, highlighting potential improvements and addressing the increasingly diverse requirements of vulnerability modelling beyond simple loss estimates.

This paper examines the equivalent SDOF-based methodology, noting that whilst it largely achieves its aim of providing reliable vulnerability functions for general application, this comes at the cost of several simplifying assumptions. The paper begins with a brief overview of equivalent SDOF modelling assumptions, followed by the widely-used approach combining fragility functions and damage-to-loss ratios to develop vulnerability functions. It then presents an alternative methodology based on storey loss functions (SLF), which is advocated here. A straightforward case study demonstrates similarities between both methodologies, emphasising the primary advantages of the SLF-based approach.

2 VULNERABILITY ASSESSMENT

2.1 Equivalent SDOF modelling

When a comprehensive numerical model of the entire structure is available, its seismic response can be characterised as intensity increases. Various analysis methods exist, ranging from linear to non-linear, static to dynamic, and SDOF to multi-degree-of-freedom (MDOF) representations. For instance, Silva et al. [7] explored several non-linear static and dynamic analysis approaches for developing fragility functions. Similarly, empirical tools such as SPO2IDA [8, 9, 10] or comparable derivatives employing more sophisticated intensity measure (IM)s [11, 12, 13] have been created. These tools might be viewed as advanced $R-\mu-T$ relation-

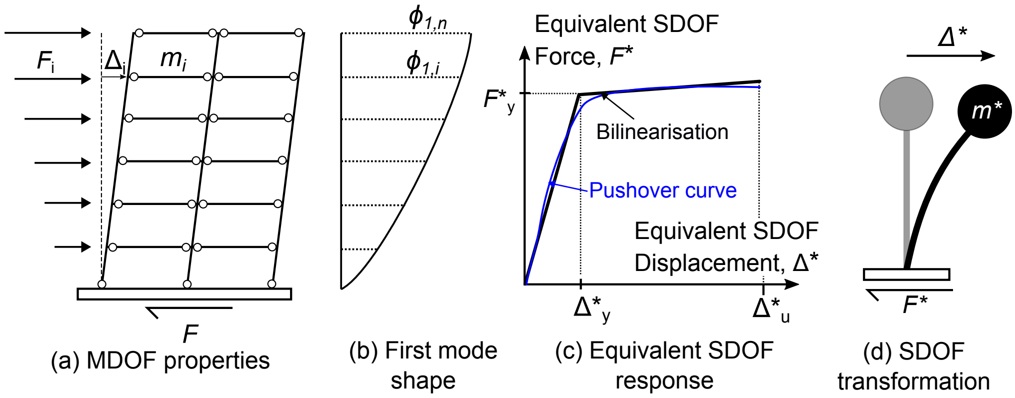

Figure 1: Basic steps in equivalent SDOF modelling

ships, similar to those initially developed by Veletsos and Newmark [14]. Naturally, a complete non-linear dynamic analysis may be conducted on MDOF models [e.g., 15], but this approach frequently proves too computationally intensive when applied at scale and challenging to implement given the quantity of structural information needed to build a detailed numerical model [e.g., 16].

A practical alternative previously adopted has been to analyse an equivalent SDOF oscillator that represents the non-linear structural behaviour. This approach features in numerous seismic design methods [e.g., 17, 18] and assessment procedures [e.g., 19, 20]. The underlying concept is that an MDOF system's seismic response can be approximated through its first mode response, as shown in Figure 1. This approximation works particularly well for low- to mid-rise structures that exhibit reasonable regularity in both plan and height.

The foundation for this approach often begins with a bi-linear representation of the structure's anticipated lateral response, typically derived from a static pushover analysis, although more detailed backbones may also be employed [e.g., 10]. This is converted to an equivalent SDOF oscillator by dividing both force and displacement values by the first mode participation factor, Γ, described in Equation 1, where m_i is the mass and $\phi_{1,i}$ is the normalised first mode shape value at floor level i. The backbone is characterised by the terms $F^* = F/\Gamma$ and $\Delta^* = \Delta/\Gamma$, where * denotes the equivalent SDOF system. The equivalent mass, m^*, is determined via Equation 2 and the period, T^*, is given by Equation 3. The ductility demand on the equivalent SDOF system is $\mu = \Delta^*/\Delta_y^*$, where Δ_y^* is the yield displacement shown in Figure 1, also denoted Sd_y. Likewise, the spectral acceleration at yield, also known as the base shear coefficient, Sa_y, may be determined by $Sa_y = F_y^*/m^*g$, where g is the acceleration due to gravity.

$$\Gamma = \frac{\sum_i m_i \phi_{1,i}}{\sum_i m_i \phi_{1,i}^2} \tag{1}$$

$$m^* = \sum_i m_i \phi_{1,i} \tag{2}$$

$$T^* = 2\pi \sqrt{\frac{m^* \Delta_y^*}{F_y^*}} \tag{3}$$

It can be noted that with a straightforward estimation of the equivalent SDOF system's period, T^*, spectral acceleration at yield, Sa_y, and ultimate ductility capacity, μ_u, a structure's response can be readily characterised through this equivalent SDOF system. This approach has formed the foundation for numerous previous studies, wherein the first mode period of structures is empirically established [e.g., 21, 22]. Additional studies have outlined methods for determining lateral strength and ductility capacity [e.g., 23] across various regions worldwide.

2.2 Storey loss function generation tool

An alternative approach to the widely-used SDOF approach is the use of SLFs, which link the engineering demand parameters (EDP)s to economic losses or decision variables decision variables (DV)s at the building storey level. To enable the wide usage of SLFs, a tool is presented. Key decisions to be made prior to using the tool include characterising the building by defining the component inventory, which is determined by the quantities, fragility, and consequence functions of the components. Additional considerations involve performance grouping of components based on their sensitivity to EDPs, identifying potential interactions between different components, selecting the number of simulations for sampling damage states and choosing the type of regression fitting for the analysis.

The process begins by identifying building characteristics such as storey count, dimensions, and usage. If unknown, SLFs can be based on a reference area and adjusted for actual size [e.g., 24, 25]. Once determined, a damageable component inventory is created, including structural and non-structural components and contents. This inventory lists item types, quantities, EDP sensitivity, and component classification. Components are grouped into three performance categories, with fragility and consequence functions often adapted from sources like FEMA P-58 [26]. For 3D buildings, the framework must be applied separately for each direction, with components oriented accordingly. In this case, components can be grouped and analysed using demands in orthogonal directions, though interactions between seismic effects aren't accounted for. If such interactions are significant, more advanced methods should be used, but for most applications, this approach suffices. While grouping the components, they are classified based on their type and the relevant EDP (e.g., peak storey drift or peak floor acceleration). The components in each group are assessed together, with their mutual demand determining the group's SLF. This classification enables loss disaggregation to identify key contributors to economic loss, as discussed by O'Reilly and Shahnazaryan [27]. This aids visualisation by identifying loss contributions from collapsing and non-collapsing cases, individual storeys, and performance groups. Similar to Ramirez and Miranda [28], components sensitive to the same EDP can be grouped to account for potential damage correlations. For instance, repairing a damaged component might require removing an undamaged one. After Monte Carlo simulations and cost computations, regression identifies the fitted SLFs. Figures 2 and 3 showcase the tool [1], which features an intuitive graphical UI designed to simplify SLF creation for seismic assessment. The following describes the key elements and functionality of the tool's use.

- Main dashboard: this area enables uploading and downloading of inputs and outputs.
- Inventory: the element inventory is presented in table format. Users can perform create, read, update and delete (CRUD) operations here. The table might include non-structural,

[1]The web-based EDP-DV prediction tool is available at https://apps.djura.it/structure/edp-dv/standard

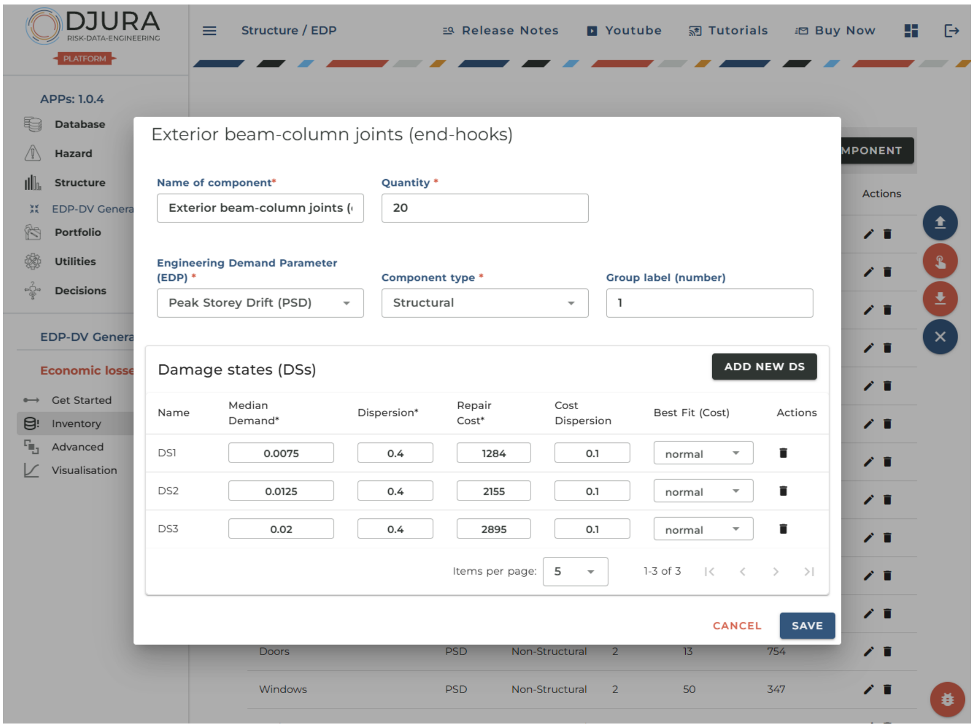

Figure 2: Overview of the interface of the SLF generation tool

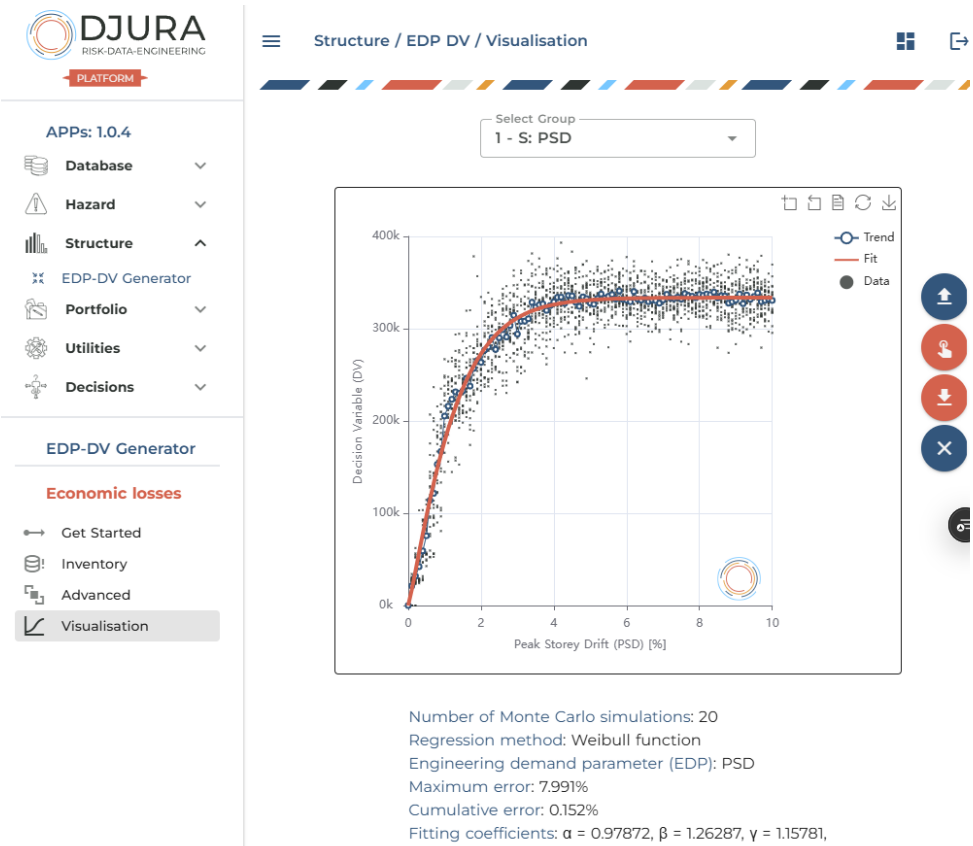

Figure 3: Example SLF visualisation

structural elements or contents characterised by quantities, EDP-sensitivity, fragility and consequence functions, as well as classifications into various performance groups.

- Advanced: the element correlation matrix updates dynamically based on changes to the element inventory. Moreover, additional calculation parameters can be modified, including: Monte Carlo simulation quantity, choice of regression function (currently supporting Weibull W. [29] and Papadopoulos et al. [25]), and various visualisation settings.
- Visualisations: users can view the generated SLFs for each performance group, alongside error metrics and fitting parameters as shown in Figure 3.

2.3 Vulnerability functions via fragility functions and damage-to-loss models

2.3.1 Fragility functions

Once the structural behaviour can be condensed to an equivalent SDOF system, it undergoes dynamic analysis using ground motion records. The key assumption is that the entire building response can be accurately depicted by a single displacement-based demand, leveraging the first-mode-dominant behaviour that remains valid for low- to mid-rise buildings. For instance, Martins and Silva [30] employed this approach for various structure types globally to develop a comprehensive fragility model, as did Villar-Vega et al. [31] for South America. Although presented in a different context, the methodology by Fajfar and Dolšek [32], later enhanced by Nafeh et al. [10], follows similar principles when assessing infilled reinforced concrete (RC) frames as they facilitate easy derivation of fragility functions. This works effectively for displacement-based demands such as roof displacement or storey drifts, which typically exhibit first-mode dominance. However, when strength-based quantities are needed (e.g., peak floor acceleration), this approach encounters difficulties since these structural demands cannot be captured solely by the first mode of response and include significant higher mode contributions. This represents a major limitation of these methods that has persisted for many years, albeit without substantial consequences.

With the response characterised across increasing seismic intensity, it is common practice to identify several key damage states (DS)s and then determine their fragility functions. These may be fitted using various statistical approaches, but the final product comprises a set of median and dispersion values for the presumed lognormal distribution of the assumed DS definition. In the research by Martins and Silva [30], for example, several displacement-based DS definitions were adopted based on the equivalent SDOF's backbone characteristics illustrated in Figure 1. These were DS1 = $0.75\Delta_y^*$, DS2 = $0.50\Delta_y^* + 0.33\Delta_u^*$, DS3 = $0.25\Delta_y^* + 0.67\Delta_u^*$, and DS4 = Δ_u^*. These were based on the recommendations of Villar-Vega et al. [31], who extended previous definitions by Lagomarsino and Giovinazzi [33], which were based on pushover curve considerations and comparisons to macro-seismic empirical data using engineering judgement.

2.3.2 Damage-to-loss models

When the median and dispersion pairs for a discrete set of fragility functions are obtained, potentially with modifications to account for additional uncertainties, it is customary to link each DS with a loss ratio through what is termed a *damage-to-loss model*, or *consequence model*. This assumes that the structure has sustained damage equivalent to a fraction of its overall replacement value at each DS, denoted as $E\left[L|DS_i\right]$ for damage state DS_i. When

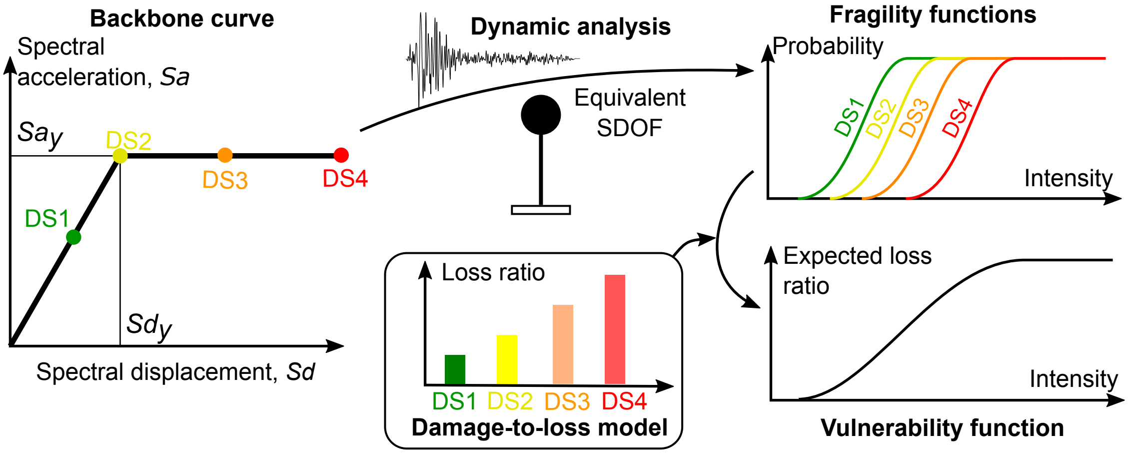

Figure 4: Development of vulnerability functions via fragility functions and damage-to-loss models

integrated with the fragility functions, the expected loss ratio versus intensity is calculated to produce the vulnerability function via Equation 4, as illustrated in Figure 4.

$$E\left[L_T|IM\right] = \sum_i E\left[L|DS_i\right] P\left[DS_i|IM\right] \tag{4}$$

Various studies have examined the development of damage-to-loss models using both analytical methods and post-earthquake observations. For instance, Kappos et al. [34] created a model for Greece with five distinct DSs, whilst HAZUS [35] published a model for the US, and Bal et al. [36] developed one for Turkey. These studies primarily relied on analytical observations with fixed ratios assigned to each DS, though some research [e.g., 15] did document the variability in these loss ratios. An earlier investigation by Di Pasquale and Goretti [37] utilised empirical data from Italy to develop a damage-to-loss model. Cosenza et al. [38] followed a comparable approach using data from the 2009 L'Aquila earthquake as part of Italy's renowned *Sismabonus* seismic risk classification guidelines [39].

A general methodology for developing vulnerability functions is outlined in D'Ayala et al. [5], and the global earthquake model (GEM) Foundation maintains an online database of available models for different countries [40]. Considerable variability exists between models, largely because each study employs slightly different criteria to identify DS exceedance. For example, Silva et al. [41] developed vulnerability functions for Portuguese RC moment frame structures using MDOF planar models with various DS criteria and associated loss ratios available in contemporary literature. Different approaches for defining DSs were presented, including manual adjustment methods to account for factors like masonry infills, highlighting the subjectivity inherent in such fragility models. A subsequent study by Martins et al. [15] further examined damage-to-loss models for vulnerability functions in Portugal. Their DSs were based on local damage criteria rather than the global criteria adopted elsewhere. For instance, DS2 was defined as when 10% or more of beams or columns yielded. However, instead of directly assigning loss ratios to each DS, they calculated expected loss ratios using repair costs based on actions needed for building recovery. This approach was classified as the "direct" method in D'Ayala et al. [5]'s guidelines, whereas Silva et al. [41]'s earlier approach exemplified the "indirect" method. A subsequent study by Martins and Silva [30] sought to provide a more standardised approach for common global building classes, employing the equivalent SDOF-based approach for developing fragility functions alongside damage-to-loss models from the online database described in Yepes-Estrada et al. [40] to derive vulnerability functions.

Whilst comparing the relative accuracy of vulnerability functions computed using these different damage-to-loss models is not this study's focus, but rather the various methodological approaches to achieve the same output, previous research has indicated they can significantly influence the resulting vulnerability functions. Although this subjectivity and sensitivity might appear as a drawback of this approach, it's important to recognise that these methods have been successfully applied at regional scales worldwide [e.g., 42, 43].

2.4 Vulnerability functions via storey loss functions

The previous section introduced a straightforward yet effective method for quantifying fragility and vulnerability models in seismic risk assessment. It highlighted the lack of consistency in discrete DS definitions across global studies, which are predominantly displacement-based and often overlook the contributions of acceleration-sensitive non-structural elements and contents. As a result, when analysing a structure's vulnerability function, it is difficult to determine the specific sources—whether displacement-based or acceleration-based demands, structural or non-structural elements—contributing to the expected economic losses. This limitation poses a significant challenge in identifying optimal retrofitting strategies to mitigate overall risk, a topic that will be explored further in later sections. To address some of these challenges in deriving vulnerability functions, this study presents an alternative approach. It builds upon previously introduced concepts, assuming the structure's seismic response can be represented by an equivalent SDOF system. However, instead of relying on discrete DSs to develop fragility functions that are then linked to a loss ratio and subsequently transformed into a vulnerability function via Equation 4, this method incorporates refinements to enhance accuracy. The advantages of these refinements will become evident in later discussions.

The general procedure is illustrated in Figure 5 and consists of two main steps: first, calculating the expected peak storey drift (PSD) and peak floor acceleration (PFA) demands at a given intensity level, and second, determining the corresponding losses at each storey level and within each damageable component group, as depicted in Figure 6. This distinction provides a more comprehensive understanding of the sources of economic losses, facilitating more effective risk-reduction strategies without significantly increasing computational effort compared to conventional approaches. It is important to acknowledge that while the proposed method is based on an equivalent SDOF system, introducing its own inherent limitations, the expected PSD and PFA demands at a given intensity can also be computed using more advanced techniques if required. Therefore, this paper presents one possible approach, while alternative methodologies remain available.

2.4.1 Peak storey drift demands

As decpited in Figure 5, the initial step involves estimating the PSD demand profile for a specific intensity. For an SDOF system with period T^*, the dynamic strength ratio (which represents the median intensity needed to surpass that level of μ) can be determined from R–μ–T relationships [14, 44, 45, 46, 8]. A fundamental assumption of these $R-\mu-T$ relationships

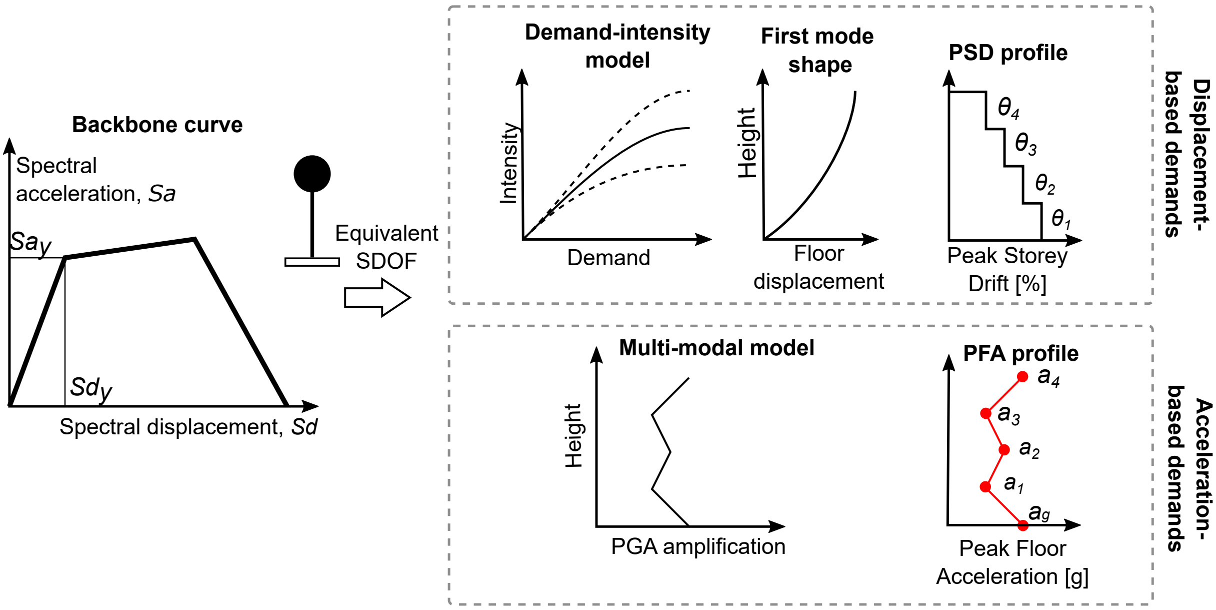

Figure 5: Storey-based approach to estimating demands

is that the IM is the spectral acceleration, $Sa(T^*)$, since R is defined as:

$$R = \frac{Sa(T^*)}{Sa_y} = \frac{F^*}{F_y^*} \tag{5}$$

During the last decade, research [e.g., 47, 48, 49, 50] has advocated a paradigm shift in seismic fragility analysis, contending that $Sa(T^*)$ exhibits several issues concerning IM efficiency and bias. Recent studies [12, 11] have instead chosen to utilise average spectral acceleration, $Sa_{avg}(T^*)$, defined as:

$$Sa_{avg}(T^*) = \left(\prod_{i=1}^{N} Sa(c_i T^*)\right)^{1/N} \tag{6}$$

where N=10 and c_i is a linearly spaced coefficient ranging from 0.2 to 2.0, although this may also be defined as 0.2 to 3.0 following Eads et al. [49]'s definition. $Sa_{avg}(T^*)$ is used in place of $Sa(T^*)$ herein but this has the consequence that the $R-\mu-T$ relationship traditionally used is now replaced by $\rho-\mu-T$ relationships, where ρ is defined as:

$$\rho = \frac{Sa_{avg}(T^*)}{Sa_y} \tag{7}$$

By applying these $\rho-\mu-T$ relationships relationships for an equivalent SDOF system with period T^*, the ductility demand, μ, can be determined at a given intensity $Sa_{avg}(T^*)$ using the tool[2] developed by Shahnazaryan and O'Reilly [11]. Once this ductility demand within the equivalent SDOF system is established for a specific intensity, the MDOF system's displacement profile can be estimated through a simple transformation factor that assumes first mode dominant behaviour for a given typology (Equation 8), whilst the corresponding peak storey drift profile, θ_i, is computed via Equation 9 where h_i represents the height of storey i. The outcome of this step is that for an assumed seismic intensity $Sa_{avg}(T^*)$, the expected PSD

[2]The web-based EDP-IM prediction tool is available at https://apps.djura.it/database/edp-im

profile, θ, across all storeys of the structure is obtained. It should be noted that this method of estimating the PSD demand profile for a given intensity represents just one possible approach, and alternatives may be adopted should the assumptions underlying these simple tools (e.g., backbone curve, ground motion records used) no longer be considered appropriate.

$$\Delta_i = \phi_{1,i}\mu\Delta_y^*\Gamma \tag{8}$$

$$\theta_i = \frac{\Delta_{i+1} - \Delta_i}{h_i} \tag{9}$$

2.4.2 Peak floor acceleration demands

The preceding section addressed the simplified estimation of PSD-based demands in a structure at a specific intensity. The corresponding PFA-based demands must also be calculated across the building height for acceleration-sensitive elements. The fundamental difference here is that the PFA at a given level, a_i, tends to contain significant contributions from several response modes. Thus, the assumption of a first mode-dominated response becomes insufficient. Nevertheless, various studies have attempted to overcome this limitation by proposing semi-empirical relationships that characterise the expected PFA profile throughout a building's height. For instance, FEMA P-58 [51] suggested a method to estimate the ratio Ω_i (see Equation 10) at each floor level i for frame, wall and braced frame structures. Other investigations [e.g., 52, 53, 54] explored approaches to more precisely quantify the complete floor response spectra of demands on non-structural elements. A recent study by Muho et al. [55], however, has proposed a technique to estimate PFA profiles based on the expected level of drift demand in the structure, which is adopted here.

The approach commences with calculating the maximum PSD throughout the structure height, θ_{max}. Given the structural typology, a functional form is identified based on the number of storeys, and a series of coefficients are determined from Muho et al. [55]. The PFA profile can then be established from the ratio Ω_i multiplied by the peak ground acceleration (PGA), a_g, where:

$$\Omega_i = \frac{a_i}{a_g} = \alpha_1 \theta_{max}^{\alpha_2} T^{\alpha_3} \tag{10}$$

The the analyst must determine whether these studies suit their specific building typology, and future developments in this area are certainly possible. A slight inconsistency in adopting this method is that the vulnerability function will be constructed for discrete values of IM=$Sa_{avg}(T^*)$. In contrast, this method by Muho et al. [55] requires a PGA value to estimate the PFA profile. This inconsistency can be resolved by simply determining the corresponding PGA value for a given $Sa_{avg}(T^*)$ by comparing their respective hazard curves. Another noteworthy aspect is that estimating PFA demands with such a simplified method requires knowledge of the building typology (e.g., moment frame). Whilst this might appear disadvantageous, as it demands additional details sometimes unnecessary for PSD demand estimation, it's worth noting that calculating the Γ parameter in Equation 1 also requires some knowledge of the first mode shape, which is likewise typology-specific.

2.4.3 Estimating repair costs

Once the expected PSD and PFA profiles are determined for a given intensity, losses can be calculated to develop a vulnerability function. This represents a key distinction in the approach outlined here, whereby rather than assuming that the structure's total economic loss can be summarised at discrete displacement-based DSs, the individual PSD and PFA demands are utilised to tabulate the expected structural and non-structural contributions to the loss in a more nuanced manner. This requires a methodology to estimate repair costs based on the anticipated level of storey drift or floor acceleration. These repair costs are dependent on the structural and non-structural damageable elements presumed to be present in the building.

Ramirez and Miranda [28] proposed a solution using what are known as SLFs, relating the level of structural demand to an expected monetary loss due to repair costs at level i as $E\left[L|NC\cap R,\theta_i\vee a_i\right]_{PG,i}$, where the terms NC and R denote that the building is in a non-collapsed state and repairable, and the operator $\vee$ denotes that either θ_i or a_i is used based on the performance group (PG) being considered. A PG in this context refers to a group of elements, either structural (S) or non-structural (NS), which are sensitive to PSD or PFA demands. Typically, the three PGs are PSD-S, PSD-NS and PFA-NS and are illustrated in Figure 6. Multiple studies have investigated the application of such SLFs [e.g., 28, 25, 56, 57], with Shahnazaryan et al. [58] developing a toolbox for their creation. These SLFs are contingent upon the assumed damageable inventory for the building and will inevitably be a function of the quantities, seismic fragility and repair costs of the various components. Shahnazaryan et al. [58] demonstrated that compared to the more detailed component-based approach advocated in P-58 [51], utilising SLFs produced essentially identical results.

The clear limitation of this approach is that the damageable components, their fragility and repair costs must be known to develop the SLFs. Typically, such information is quite abundant when studying the North American context, with databases in P-58 [51] providing much of the necessary information. Analysts should be cautious when applying such databases and data to other regional contexts where structural and non-structural components may perform differently, or where repair costing and quantities information varies significantly. However, a recent investigation by Nafeh and O'Reilly [59] analysed over 105 infilled reinforced concrete building models, varying the number of storeys, global dimensions, occupancy type, structural typology and other specific architectural features, such as infill locations. They discovered that for a given typology and assumed building occupancy type (e.g., residential, commercial), the SLFs' *relative* trend tends to be comparatively stable, though their absolute values may vary depending on the storey value. This occurs because repair costs tend to be broadly similar and essentially scaled up and down according to the damageable inventory's relative magnitude. O'Reilly et al. [60] suggested using *generalised* SLFs, whereby the functions are normalised by their total PG value at each storey. These generalised SLFs are defined as follows:

$$E\left[\tilde{L}|NC\cap R,\theta_i\vee a_i\right]_{PG,i}=\frac{E\left[L|NC\cap R,\theta_i\vee a_i\right]_{PG,i}}{\sum_{PG}E\left[L|NC\cap R,\infty\right]_{PG,i}} \tag{11}$$

where $E\left[L|NC\cap R,\infty\right]_{PG,i}$ represents the expected loss among all components of a PG at storey level i at infinite demand. This means that the total value of $E\left[\tilde{L}|NC\cap R,\theta_i\vee a_i\right]_{PG,i}$ for all PG at each level i should sum to unity. Esmaili et al. [57] briefly mentioned a similar approach for use in regional analysis, although in that study the SLFs are normalised by the replacement cost of each storey, whose exact computation was not clear. With a set of generalised SLFs, which ultimately represent the trend in accumulation of losses for increased PSD and PFA demands with intensity, a user can specify their different PG's relative contribution to

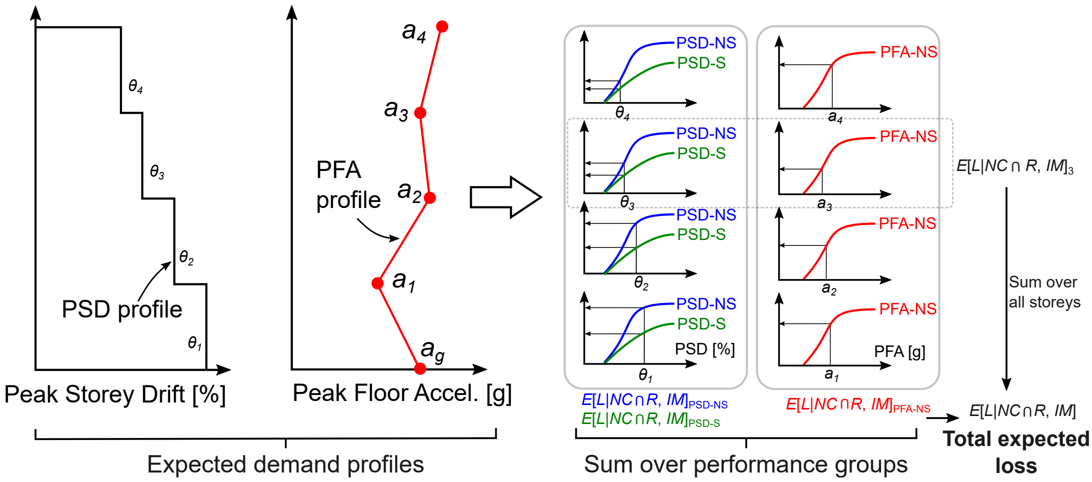

Figure 6: Estimating expected repair costs using SLFs

$E\left[\tilde{L}|NC \cap R, \theta_i \vee a_i\right]_{PG,i}$ and proceed from there. Summing these together for each storey, the total losses due to repair costs, $E\left[L|NC \cap R, IM\right]$, is then computed at a given IM value as:

$$E\left[L|NC \cap R, IM\right] = \sum_{i} \sum_{PG} E\left[L|NC \cap R, \theta_i(IM) \vee a_i(IM)\right]_{PG,i} \tag{12}$$

where the θ_i and a_i are calculated for each level of IM, as described in previous sections. This means that an analyst may simply adopt generalised SLFs from an established database, provided they accept that the relative trend of repair costs with increasing storey drift or floor acceleration truly represents their building typology and region of interest. These databases could be expanded in future studies, similar to current practice with damage-to-loss models. They would offer the additional advantage of more detailed information within this model using actual demand parameters, which can be modified if necessary.

2.4.4 Assembling the vulnerability function

The preceding section outlined how the expected building loss due to repairs, denoted as $E\left[L|NC \cap R, IM\right]$, can be estimated. It's crucial to remember that this represents just one potential loss source. Other significant sources that should be considered include the possibility of building collapse or damage so extensive that demolition rather than repair is required. In essence, economic loss can be viewed as the sum of three mutually exclusive, collectively exhaustive events: non-collapse requiring repair (R), non-collapse requiring demolition (D) and total replacement due to collapse (C). When combined, the vulnerability function is assembled as follows:

$$\begin{aligned} E\left[L_T|IM\right] = &\underbrace{E\left[L|NC \cap R, IM\right]\left(1 - P\left[D|NC, IM\right]\right)\left(1 - P\left[C|IM\right]\right)}_{\text{Non-collapse requiring repair}} + \\ &\underbrace{E\left[L|NC \cap D\right] P\left[D|NC, IM\right]\left(1 - P\left[C|IM\right]\right)}_{\text{Non-collapse requiring demolition}} + \\ &\underbrace{E\left[L|C\right] P\left[C|IM\right]}_{\text{Collapse requiring replacement}} \end{aligned} \tag{13}$$

where $P\left[D|NC,IM\right]$ represents the probability of requiring demolition for a non-collapsed structure. Ramirez and Miranda [61] provided a means of estimating this based on expected residual drifts in the structure, though further research is needed to understand this issue more thoroughly. Additionally, demolition may be the simpler option if the owner considers it more worthwhile to begin with a new building rather than repair the existing one. For instance, Kim et al. [62] discussed this scenario for New Zealand following the 2011-2012 Canterbury earthquakes, where several factors were identified as playing significant roles. However, if this issue can be disregarded and the non-collapsed building is always assumed to be repairable (i.e., $P\left[D|NC,IM\right]=0$), Equation 13 simplifies to:

$$E\left[L_T|IM\right]=\underbrace{E\left[L|NC,IM\right]\left(1-P\left[C|IM\right]\right)}_{\text{Non-collapse requiring repair}}+\underbrace{E\left[L|C\right]P\left[C|IM\right]}_{\text{Collapse requiring replacement}} \tag{14}$$

where the $P\left[C|IM\right]$ denotes the collapse probability at the given intensity level. This may be computed directly from the collapse fragility function provided by the EDP-IM prediction tool[2] previously described. It is worth noting that integrating the collapse fragility function with seismic hazard enables the determination of collapse risk, similar to how the vulnerability function is used to derive expected (or average) annual losses.

3 CASE STUDY EXAMPLE

A case study application was carried out for a comparative assessment between fragility-based and SLF-based approaches. Some additional parameters are necessary for the application of the SLF-based approach, which include the number of storeys, storey heights, structural typology, occupancy type. For simplicity, we used an RC moment-resisting frame (MRF) building with 4 storeys (ground floor 3.5m high, others 3.0m). The backbone curve had these properties: 1.0s secant-to-yield period, 4.0 ductility, 0.2 base shear coefficient, 0.02 hardening ratio and -0.5 softening slope. Importantly, the equivalent SDOF's backbone curve was used in the fragility-based approach. To maintain consistency for comparison, the reqsulting equivalent SDOF's backbone curve was used in the fragility-based approach.

The equivalent SDOF oscillator ($T^*=1s$) was modelled with OpenSeesPy's [63] *Hysteretic* material for the fragility-based approach, with 5.0% Rayleigh damping. Both hardening and degrading branches were included, creating a tri-linear degrading backbone curve shown in Figure 7a with PSD-based DSs marked. This curve was considered to be a better reflection of common structural systems encountered in seismic design and assessment over a simpler bi-linear model without degradation.

3.1 Fragility functions and loss ratios approach

Vulnerability assessment was conducted using fragility functions and the damage-to-loss model of Martins and Silva [30] (Figure 7b). The damage-to-loss model utilised four DSs ranging from slight (DS1) to complete damage (DS4). To account for damage onset in non-structural elements such as infill walls, slight damage was assumed to begin at 75% of the yielding displacement, whilst complete damage was assumed at the structure's ultimate displacement capacity. Intermediate DSs were positioned at even intervals between the initial and ultimate DS. To derive the fragility functions, non-linear time history analyses were performed following a cloud analysis approach [64]. As previously noted, $Sa_{avg}(T^*=1.0s)$ was selected as the IM

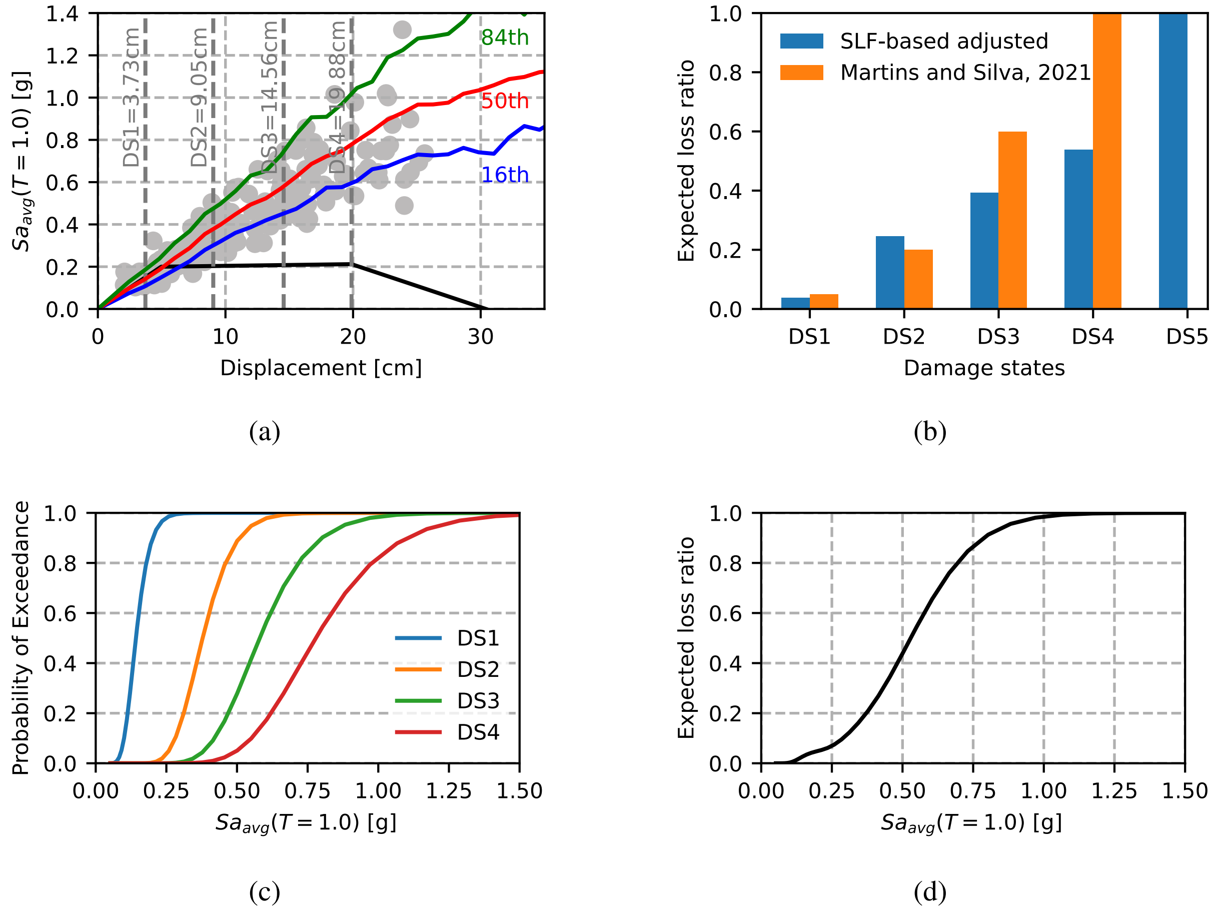

Figure 7: (a) Damage-to-loss models adopted; (b) backbone curve, cloud analysis results, and EDP-IM (https://apps.djura.it/database/edp-im) 16^{th}, 50^{th} and 84^{th} percentile predictions; (c) fragility functions; and (d) vulnerability function of fragility-based assessment

for the case study application, although this was not strictly required. Record selection was necessary to perform cloud analysis. Following Martins and Silva [30], ten bins of IM were established between 0.1g and 2.0g, with 30 records randomly selected for each bin from the NGA-West2 database [65]. This resulted in 300 selected records, with some records scaled by a maximum factor of 2.0 to populate the more intense IM bins. Figure 7a illustrates the cloud analysis results, showing that most records exceeding an $Sa_{avg}(T^* = 1.0s)$ of 1.0g caused numerical instabilities due to lateral collapse. With the defined damage-to-loss model, the fragility function parameters were calculated using the maximum likelihood estimation method and are presented in Figure 7c. As previously discussed, once the discrete set of fragility functions associated with each DS and corresponding expected loss ratio were obtained, the vulnerability function was calculated via Equation 4 and is depicted in Figure 7d.

3.2 SLF-based approach

The generalised SLFs, developed using the tool[1] presented in 2.2 were used for vulnerability assessment. The developed curves, representing $E\left[\tilde{L}|NC \cap R, \theta_i \vee a_i\right]_{PG,i}$ in Equation 11, are shown in Figure 8, and are simply adopted from an example presented in Shahnazaryan

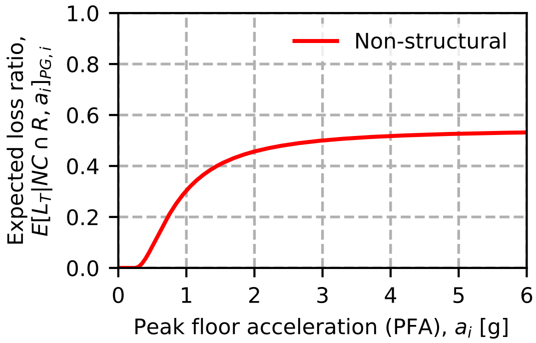

(a)

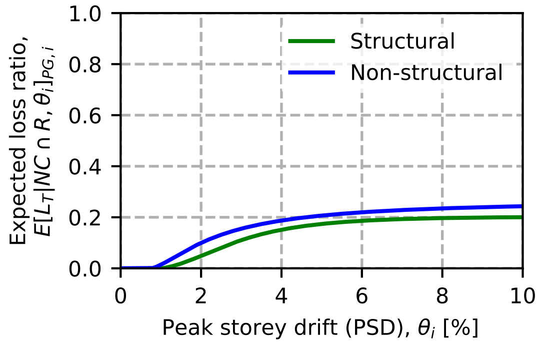

(b)

Figure 8: Generalised SLFs for the case study structure: (a) PFA-sensitive, and (b) PSD-sensitive

et al. [58]. It is important to note that these SLFs are not intended to be representative of the specific building typology and occupancy examined here, but rather serve as an arbitrary set of functions for demonstration purposes. The SLFs were assumed to have different relative values at each storey (i.e, $\sum_{PG} E\left[L|NC \cap R, \infty\right]_{PG,i}$ from Equation 11) with the ratios 2:3:3:3.5 for PSD-NS; 3:2.5:2.5:1.5 for PSD-S; and 4:1:1:2 for PFA-NS used to provide variability and were all normalised to a total value of unity for the entire building.

To identify the demand-intensity model through the EDP-IM tool[2], the equivalent SDOF representation was derived following the previously outlined procedure. Figure 7a also includes the EDP-IM predictions for displacement and IM, which are essentially identical, meaning that non-linear dynamic analysis with ground motion records is not required. Using this estimated value of μ for a given $Sa_{avg}(T^* = 1.0s)$ value, the PSD profile was estimated from Equation 9. For floor accelerations, the PFA profile was estimated using Equation 10.

Consequently, the PSDs and PFAs associated with different intensity levels enabled the calculation of repair costs using the SLFs of Figure 8 and Equation 12. It should be noted that these simplified methods to estimate the PSD and PFA demands are generally based on empirical formulae calibrated from past numerical analysis results. This may introduce additional uncertainties into calculations, particularly when extending the SLF-based approach to large-scale risk analysis. However, the magnitude of these uncertainties relative to other sources is not expected to be significant. Furthermore, these estimation approaches can be seamlessly substituted in the present approach for more refined means of estimating demands. Other prominent sources of loss include non-collapse requiring demolition and total replacement costs due to collapse. Although demolition costs could be easily incorporated by considering residual drifts or assuming a demolition capacity of a structure, as suggested in Ramirez and Miranda [28], these were excluded from this case study application to maintain a comparative basis with the fragility-based approach. Regarding losses associated with structural collapse, the collapse fragility function was estimated using the EDP-IM prediction tool[2], which was then used to estimate the probability of collapse at each IM level. The resulting vulnerability function was calculated using Equation 14 and is plotted in Figure 9. Also shown is the disaggregation of the vulnerability function for each PG along with the collapse contribution.

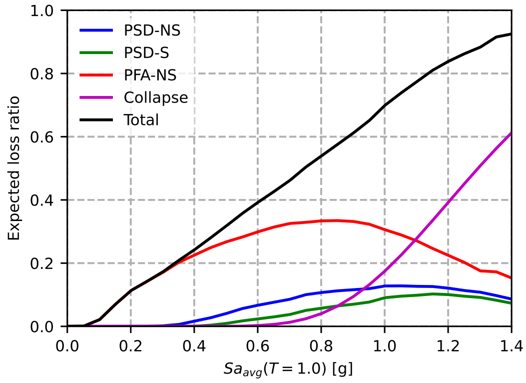

Figure 9: Vulnerability functions showing the breakdown between different contributors following the SLF-based approach

3.3 Comparison of results

The vulnerability functions obtained through the fragility- and SLF-based approaches are compared here to examine the similarities and crucial differences between the two methods. Figure 10 presents this comparison, where the immediate observation is that the two methods differ notably, albeit within the same order of magnitude. This is not surprising given that the damage-to-loss models used to develop these vulnerability functions differed in both cases. The structural demands were identical, however, as illustrated in Figure 7a; hence, any discrepancy stems from the difference in loss model. One immediate observation is that the SLF-based vulnerability function is considerably higher at lower intensities than the fragility-based function. This simply reflects the different loss models in this specific scenario and does not suggest that SLF-based functions are generally expected to be higher.

To provide a more compatible comparison of the two methods, the DS loss ratios required for the fragility-based method were back-calculated from the SLF-based approach's results. That is, the fragility functions shown in Figure 7c were integrated with the red line shown in Figure 10. This is described by Equation 15 and the resulting loss ratios are shown in Figure 7b as *SLF-based adjusted*. An additional DS of collapse was added with a loss ratio of 1.0 for consistency. The vulnerability function using these adjusted loss ratios is shown in Figure 10 alongside the original fragility-based and SLF-based approaches. Despite the stark disparity between the vulnerability functions of fragility-based and SLF-based approaches, this does not necessarily reflect negatively on either methodology, as the initial set of loss ratios was not consistent with the SLF functions (Figure 8) employed. This is emphasised when compatible loss ratios were derived and used within the fragility-based method, shown as the green line. Some discrepancy remains, but further investigation revealed this was a consequence of using just four DSs in the fragility-based method. If many more DSs were added, the fragility-based and SLF-based approaches' results (i.e., the red and green lines in Figure 10) would coincide perfectly. Hence, the discrepancy shown in Figure 10 results from discretisation error and may be theoretically reduced by adding further DSs. However, doing so would likely encounter practical issues beyond the scope of interest for this study. The key message here is that for a compatible set of loss ratios and a sufficient number of DSs, the discrete fragility-based approach theoretically converges towards the more continuous SLF-based approach. This is an encouraging observation as it essentially means the two are equivalent, with one offering more

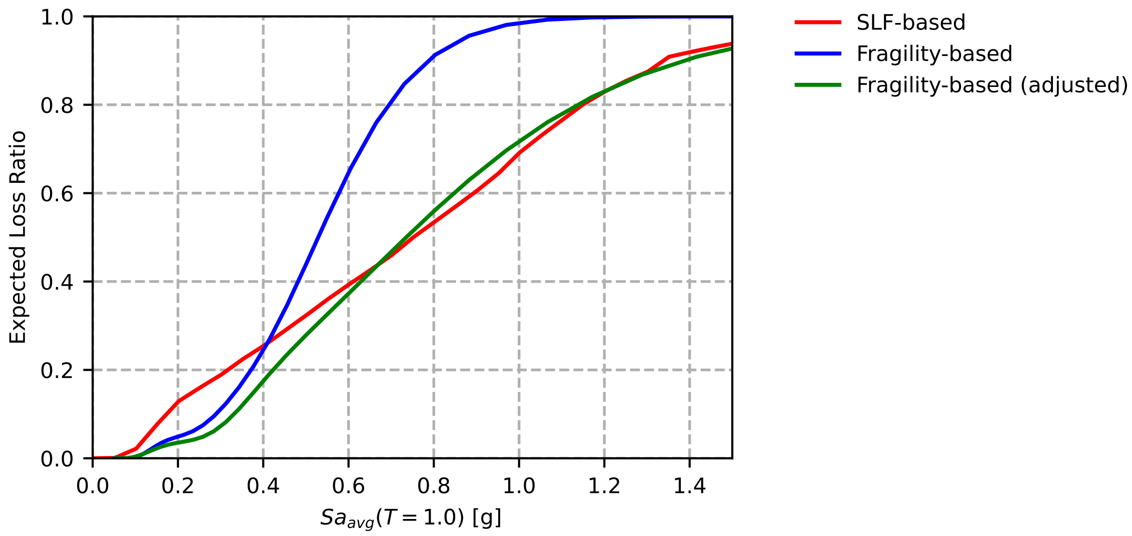

Figure 10: Comparison of the fragility-based and SLF-based vulnerability functions

outputs and insight than the other.

$$E\left[L|DS_i\right] = \int_0^{+\infty} P\left[DS_i|IM\right]\left(\frac{dE\left[L_T|IM\right]}{dIM}\right)dIM \tag{15}$$

To further highlight the enhanced output offered via the SLF-based approach, Figure 11a provides the relative contributions of different PGs and collapse losses to the vulnerability functions as a function of IM. At lower levels of IM, repair (non-collapse) losses, particularly attributable to PFA-sensitive non-structural PG, emerge as the primary contributors. As intensity increases, the contributions from PSD-sensitive non-structural and structural PGs gradually rise while remaining relatively stable. Conversely, the contribution from collapse to expected loss ratio starts increasing at mid-to-high intensities, eventually becoming the dominant factor in overall loss. Another significant advantage of the SLF-based approach lies in its ability to disaggregate losses along the height of the building, as shown in Figure 11b. Here it is clear which PG contributes most to the losses at each individual level, not merely for the entire building. Again, this specific example has been chosen to illustrate the approach's potential and does not suggest this is the expected loss distribution for this typology. Only through accurate and more specific data will it be possible to observe general trends. The point is to demonstrate some key benefits of using the proposed SLF-based approach compared to the fragility-based approach of SDOF systems, as disaggregation of losses allows designers or stakeholders to identify and address vulnerable components within the building without requiring extensive analysis.

4 SUMMARY AND CONCLUSIONS

This paper presented a comparative study of two methodologies for developing vulnerability functions applicable to regional seismic risk modelling. These methodologies were underpinned by analytical methods and incorporated several key assumptions to ensure widespread applicability and computational efficiency. The first methodology was predicated on fragility analysis of displacement-based demands on an equivalent single-degree-of-freedom (SDOF) model

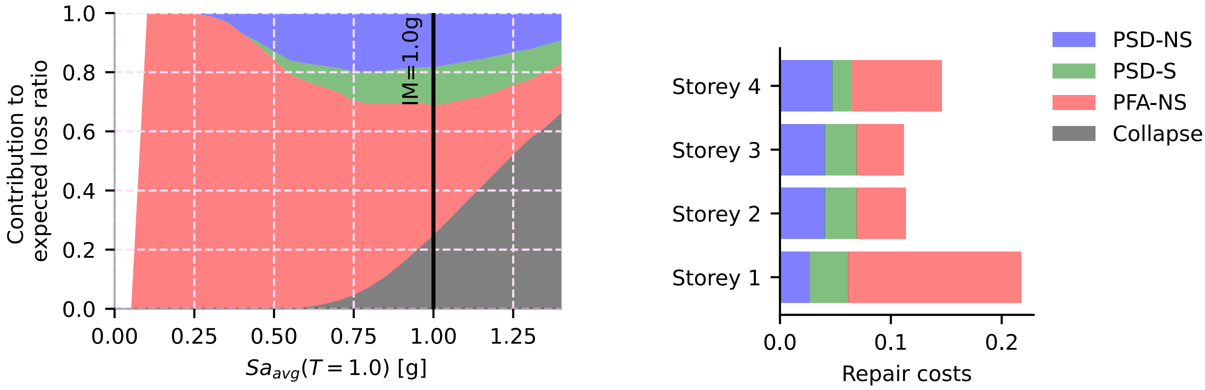

(a) (b)

Figure 11: (a) Relative contribution to expected loss with respect to increasing IM, and (b) repair cost contributors along the structure's height at the IM of 1.0g

which, when combined with loss ratios, yields vulnerability functions. A second, alternative approach described herein employs an equivalent SDOF model to estimate both displacement- and acceleration-based demands at each building level. The integration of these demands with storey loss functions (SLF)s, easily derivable through https://apps.djura.it/structure/edp-dv/standard, facilitates the estimation of vulnerability at each storey and, ultimately, the vulnerability function of the entire building. Both methodologies were elucidated in detail, and a comparative case study was presented to examine their similarities and differences.

Based on the research presented herein, the following conclusions may be drawn:

- The SLF-based approach represents a more detailed and robust methodology compared to the widely-utilised fragility and damage-to-loss ratio-based approach. Although the SLF-based approach offers greater detail, it does not incur the burden of excessive additional computation or effort. Indeed, when simplified, the SLF-based approach can be reduced to yield essentially the same result as the fragility-based approach.

- The SLF-based approach directly considers both peak storey drift (PSD)- and peak floor acceleration (PFA)-based demands at all storeys of the building. This decomposition permits a more detailed consideration of non-structural elements and identifies which performance groups at which building locations contribute most significantly to the expected loss.

- The issues of collapse and demolition are addressed more directly, which can prove valuable for decision-making beyond economic losses, such as estimating casualties or determining when retrofitting interventions may be futile.

Overall, this extension from the existing to the proposed approach entails minimal additional computational cost whilst representing an enhanced level of quality in the output decision variables employed in regional seismic risk assessment.

5 ACKNOWLEDGEMENTS

The work presented in this paper has been developed within the framework of the project "Dipartimenti di Eccellenza 2023-2027", funded by the Italian Ministry of Education, University and Research at IUSS Pavia. An academic license was used to perform the SLF creation and demand estimation through the online platform at www.djura.it.

References

[1] Gian Michele Calvi, Rui Pinho, Guido Magenes, J. J. Bommer, L. F. Restrepo-Vélez, and Helen Crowley. Development of seismic vulnerability assessment methodologies over the past 30 years. *ISET Journal of Earthquake Technology*, 43(3):75–104, 2006. URL `http://home.iitk.ac.in/{~}vinaykg/Iset472.pdf`.

[2] Gian Michele Calvi. A displacement-based approach for vulnerability evaluation of classes of buildings. *Journal of Earthquake Engineering*, 3(3):411–438, 1999. ISSN 13632469. doi: 10.1080/13632469909350353.

[3] Helen Crowley, Rui Pinho, and Julian J. Bommer. A Probabilistic Displacement-based Vulnerability Assessment Procedure for Earthquake Loss Estimation. *Bulletin of Earthquake Engineering*, 2(2):173–219, 2004. ISSN 1570-761X. doi: 10.1007/s10518-004-2290-8. URL `http://link.springer.com/10.1007/s10518-004-2290-8`.

[4] Barbara Borzi, Helen Crowley, and Rui Pinho. Simplified Pushover-Based Earthquake Loss Assessment (SP-BELA) Method for Masonry Buildings. *International Journal of Architectural Heritage*, 2(4):353–376, nov 2008. ISSN 1558-3058. doi: 10.1080/15583050701828178. URL `http://www.tandfonline.com/doi/abs/10.1080/15583050701828178`.

[5] D D'Ayala, A Meslem, Dimitrios Vamvatsikos, Keith Porter, Tiziana Rossetto, and Vitor Silva. Guidelines for Analytical Vulnerability Assessment of Low/Mid-Rise Buildings. Technical report, GEM TECHNICAL REPORT 2014-12 V1.0.0, 2014.

[6] Vitor Silva, Sinan Akkar, Jack Baker, Paolo Bazzurro, José Miguel Castro, Helen Crowley, Matjaz Dolsek, Carmine Galasso, Sergio Lagomarsino, Ricardo Monteiro, Daniele Perrone, Kyriazis Pitilakis, and Dimitrios Vamvatsikos. Current Challenges and Future Trends in Analytical Fragility and Vulnerability Modeling. *Earthquake Spectra*, 35(4):1927–1952, nov 2019. ISSN 8755-2930. doi: 10.1193/042418EQS101O. URL `http://journals.sagepub.com/doi/10.1193/042418EQS101O`.

[7] V. Silva, Helen Crowley, H. Varum, R. Pinho, and R. Sousa. Evaluation of analytical methodologies used to derive vulnerability functions. *Earthquake Engineering & Structural Dynamics*, 43(2):181–204, feb 2014. ISSN 00988847. doi: 10.1002/eqe.2337. URL `http://doi.wiley.com/10.1002/eqe.2337`.

[8] Dimitrios Vamvatsikos and C. Allin Cornell. Direct Estimation of Seismic Demand and Capacity of Multidegree-of-Freedom Systems through Incremental Dynamic Analysis of Single Degree of Freedom Approximation. *Journal of Structural Engineering*, 131(4): 589–599, 2005. ISSN 0733-9445. doi: 10.1061/(asce)0733-9445(2005)131:4(589).

[9] Georgios Baltzopoulos, Roberto Baraschino, Iunio Iervolino, and Dimitrios Vamvatsikos. SPO2FRAG: software for seismic fragility assessment based on static pushover. *Bulletin of Earthquake Engineering*, 2017. ISSN 1573-1456. doi: 10.1007/s10518-017-0145-3.

[10] Al Mouayed Bellah Nafeh, Gerard J. O'Reilly, and Ricardo Monteiro. Simplified seismic assessment of infilled RC frame structures. *Bulletin of Earthquake Engineering*, 18 (4):1579–1611, mar 2020. ISSN 1570-761X. doi: 10.1007/s10518-019-00758-2. URL `http://link.springer.com/10.1007/s10518-019-00758-2`.

[11] Davit Shahnazaryan and Gerard John O'Reilly. Next-generation non-linear and collapse prediction models for short- to long-period systems via machine learning methods. *Engineering Structures*, 2024. doi: 10.1016/j.engstruct.2024.117801.

[12] Al Mouayed Bellah Nafeh and Gerard John O'Reilly. Unbiased simplified seismic fragility estimation of non-ductile infilled RC structures. *Soil Dynamics and Earthquake Engineering*, 157:107253, jun 2022. ISSN 02677261. doi: 10.1016/j.soildyn.2022.107253. URL `https://linkinghub.elsevier.com/retrieve/pii/S0267726122001026`.

[13] Savvinos Aristeidou, Karim Tarbali, and Gerard J O'Reilly. A ground motion model for orientation-independent inelastic spectral displacements from shallow crustal earthquakes. *Earthquake Spectra*, 39(3):1601–1624, aug 2023. ISSN 8755-2930. doi: 10.1177/87552930231180228. URL `http://journals.sagepub.com/doi/10.1177/87552930231180228https://journals.sagepub.com/doi/10.1177/87552930231180228`.

[14] A. S. Veletsos and N. M. Newmark. Effect of inelastic behavior on the response of simple systems to earthquake motions. In *Proceedings of the third world conference on earthquake engineering*, pages 895–912, 1960.

[15] Luís Martins, Vítor Silva, Mário Marques, Helen Crowley, and Raimundo Delgado. Development and assessment of damage-to-loss models for moment-frame reinforced concrete buildings. *Earthquake Engineering & Structural Dynamics*, 45(5):797–817, dec 2015. doi: 10.1002/eqe.2687.

[16] Gerard J. O'Reilly, Daniele Perrone, Matthew Fox, Ricardo Monteiro, and Andre Filiatrault. Seismic assessment and loss estimation of existing school buildings in Italy. *Engineering Structures*, 168:142–162, aug 2018. ISSN 01410296. doi: 10.1016/j.engstruct.2018.04.056. URL `http://linkinghub.elsevier.com/retrieve/pii/S0141029617325610`.

[17] CEN. Eurocode 8: Design of Structures for Earthquake Resistance - Part 1: General Rules, Seismic Actions and Rules for Buildings (EN 1998-1:2004). European standard, Comité Européen de Normalisation, Brussels, 2004.

[18] ASCE 7-22. *Minimum Design Loads for Buildings and Other Structures*. American Society of Civil Engineers, 2022. ISBN 9780784479964.

[19] M. J. N. Priestley. Displacement-Based Seismic Assessment of Reinforced Concrete Buildings. *Journal of Earthquake Engineering*, 1(1):157–192, jan 1997. ISSN 1363-2469. doi: 10.1080/13632469708962365. URL `http://dx.doi.org/10.1080/13632469708962365`.

[20] Peter Fajfar. A Nonlinear Analysis Method for Performance-Based Seismic Design. *Earthquake Spectra*, 16(3):573–592, 2000. ISSN 87552930. doi: 10.1193/1.1586128.

[21] H. Crowley and R. Pinho. Period-Height Relationship for Existing European Reinforced Concrete Buildings. *Journal of Earthquake Engineering*, 8(Supp1):93–119, jan 2004. ISSN 1363-2469. doi: 10.1080/13632460409350522. URL `http://www.tandfonline.com/doi/abs/10.1080/13632460409350522`.

[22] Sergio Ruggieri, Andrea Fiore, and Giuseppina Uva. A New Approach to Predict the Fundamental Period of Vibration for Newly-designed Reinforced Concrete Buildings. *Journal of Earthquake Engineering*, 26(13):6943–6968, oct 2022. ISSN 1363-2469. doi: 10.1080/13632469.2021.1961929. URL `https://www.tandfonline.com/doi/full/10.1080/13632469.2021.1961929`.

[23] Helen Crowley, Venetia Despotaki, Vitor Silva, Jamal Dabbeek, Xavier Romao, Nuno Pereira, Jose Miguel Castro, James Daniell, Enes Veliu, Huseyin Bilgin, Christoph Adam, Manya Deyanova, Naida Ademovic, Josip Atalic, Evi Riga, Anna Karatzetzou, Bjarni Bessason, Veronika Shendova, Alexandru Tiganescu, Dragos Toma-Danila, Zeljko Zugic, Sinan Akkar, and Ufuk Hancilar. Model of seismic design lateral force levels for the existing reinforced concrete European building stock. *Bulletin of Earthquake Engineering*, 19(7):2839–2865, may 2021. ISSN 1570-761X. doi: 10.1007/s10518-021-01083-3. URL `https://link.springer.com/10.1007/s10518-021-01083-3`.

[24] G. J. O'Reilly G. Perrone, D. Cardone and T. J. Sullivan. Developing a direct approach for estimating expected annual losses of italian buildings. *Journal of Earthquake Engineering*, 26(1):1–32, 2022. doi: 10.1080/13632469.2019.1657988. URL `https://doi.org/10.1080/13632469.2019.1657988`.

[25] Athanasios N. Papadopoulos, Dimitrios Vamvatsikos, and Athanasia K. Kazantzi. Development and Application of FEMA P-58 Compatible Story Loss Functions. *Earthquake Spectra*, 35(1):95–112, feb 2019. ISSN 8755-2930. doi: 10.1193/102417EQS222M. URL `http://journals.sagepub.com/doi/10.1193/102417EQS222M`.

[26] FEMA. FEMA P58-3. Seismic Performance Assessment of Buildings Volume 3 - Performance Assessment Calculation Tool (PACT). Technical report, Federal Emergency Management Agency, Washington, D.C., 2012.

[27] Gerard J O'Reilly and Davit Shahnazaryan. On the utility of story loss functions for regional seismic vulnerability modeling and risk assessment. *Earthquake Spectra*, 40(3): 1933–1955, 2024. doi: 10.1177/87552930241245940.

[28] C. M. Ramirez and Eduardo Miranda. Building Specific Loss Estimation Methods & Tools for Simplified Performance Based Earthquake Engineering. *Blume Report No. 171*, 2009.

[29] Weibull W. *The Statistical Theory of the Strength of Materials*. Generalstabens Litografiska Anstalts Förlag, Stockholm, 151 edition, 1939.

[30] Luís Martins and Vítor Silva. Development of a fragility and vulnerability model for global seismic risk analyses. *Bulletin of Earthquake Engineering*, 19(15):6719–6745, dec 2021. ISSN 1570-761X. doi: 10.1007/s10518-020-00885-1. URL https://link.springer.com/10.1007/s10518-020-00885-1.

[31] Mabé Villar-Vega, Vitor Silva, Helen Crowley, Catalina Yepes, Nicola Tarque, Ana Beatriz Acevedo, Matías A. Hube, Coronel D. Gustavo, and Hernán Santa María. Development of a fragility model for the residential building stock in South America. *Earthquake Spectra*, 33(2):581–604, 2017. ISSN 87552930. doi: 10.1193/010716EQS005M.

[32] Peter Fajfar and Matjaž Dolšek. A practice-oriented estimation of the failure probability of building structures. *Earthquake Engineering & Structural Dynamics*, 41(3):531–547, mar 2012. ISSN 00988847. doi: 10.1002/eqe.1143. URL http://doi.wiley.com/10.1002/eqe.1143.

[33] Sergio Lagomarsino and Sonia Giovinazzi. Macroseismic and mechanical models for the vulnerability and damage assessment of current buildings. *Bulletin of Earthquake Engineering*, 4(4):415–443, nov 2006. ISSN 1570-761X. doi: 10.1007/s10518-006-9024-z. URL http://link.springer.com/10.1007/s10518-006-9024-z.

[34] Andreas J. Kappos, Georgios Panagopoulos, Christos Panagiotopoulos, and Gregorios Penelis. A hybrid method for the vulnerability assessment of R/C and URM buildings. *Bulletin of Earthquake Engineering*, 4(4):391–413, nov 2006. ISSN 1570-761X. doi: 10.1007/s10518-006-9023-0. URL http://link.springer.com/10.1007/s10518-006-9023-0.

[35] HAZUS. Multi-Hazard Loss Estimation Methodology - Earthquake Model. Technical report, Federal Emergency Management Agency, Washington, DC, 2003.

[36] İ. Engin Bal, Helen Crowley, Rui Pinho, and F. Gülten Gülay. Detailed assessment of structural characteristics of Turkish RC building stock for loss assessment models. *Soil Dynamics and Earthquake Engineering*, 28(10-11):914–932, oct 2008. ISSN 02677261. doi: 10.1016/j.soildyn.2007.10.005. URL https://linkinghub.elsevier.com/retrieve/pii/S0267726107001340.

[37] G Di Pasquale and Agostino Goretti. Vulnerabilita funzionale ed economica degli edifici residenziali colpiti dai recenti eventi sismici italiani. In *Proceedings of the 10th national conference L'ingegneria Sismica in Italia*, Potenza-Matera, Italy, 2001.

[38] Edoardo Cosenza, Ciro Del Vecchio, Marco Di Ludovico, Mauro Dolce, Claudio Moroni, Andrea Prota, and Emanuele Renzi. The Italian guidelines for seismic risk classification of constructions: technical principles and validation. *Bulletin of Earthquake Engineering*, 16(12):5905–5935, dec 2018. ISSN 1570-761X. doi: 10.1007/s10518-018-0431-8. URL http://link.springer.com/10.1007/s10518-018-0431-8.

[39] Decreto Ministeriale. Linee Guida per la Classificazione del Rischio Sismico delle Costruzioni - 58/2017. Technical report, Il ministero delle infrastrutture e dei trasporti, Rome, Italy, 2017.

[40] Catalina Yepes-Estrada, Vitor Silva, Tiziana Rossetto, Dina D'Ayala, Ioanna Ioannou, Abdelghani Meslem, and Helen Crowley. The Global Earthquake Model Physical Vulnerability Database. *Earthquake Spectra*, 32(4):2567–2585, nov 2016. ISSN 8755-2930. doi: 10.1193/011816EQS015DP. URL `http://journals.sagepub.com/doi/10.1193/011816EQS015DP`.

[41] Vitor Silva, Helen Crowley, Humberto Varum, Rui Pinho, and Luis Sousa. Investigation of the characteristics of Portuguese regular moment-frame RC buildings and development of a vulnerability model. *Bulletin of Earthquake Engineering*, 13(5):1455–1490, sep 2014. ISSN 1570-761X. doi: 10.1007/s10518-014-9669-y. URL `http://link.springer.com/10.1007/s10518-014-9669-y`.

[42] Vitor Silva, Desmond Amo-Oduro, Alejandro Calderon, Catarina Costa, Jamal Dabbeek, Venetia Despotaki, Luis Martins, Marco Pagani, Anirudh Rao, Michele Simionato, Daniele Viganò, Catalina Yepes-Estrada, Ana Acevedo, Helen Crowley, Nick Horspool, Kishor Jaiswal, Murray Journeay, and Massimiliano Pittore. Development of a global seismic risk model. *Earthquake Spectra*, 36(1_suppl):372–394, oct 2020. ISSN 8755-2930. doi: 10.1177/8755293019899953. URL `http://journals.sagepub.com/doi/10.1177/8755293019899953`.

[43] Vitor Silva and Nick Horspool. Combining usgs shakemaps and the openquake-engine for damage and loss assessment. *Earthquake Engineering & Structural Dynamics*, 48(6):634–652, 2019. doi: https://doi.org/10.1002/eqe.3154. URL `https://onlinelibrary.wiley.com/doi/abs/10.1002/eqe.3154`.

[44] N. M. Newmark and John F. Hall. Earthquake specta design. Technical report, Earthquake Engineering Research Institute, Berkeley, California, 1982.

[45] Tomaž Vidic, Peter Fajfar, and Matej Fischinger. Consistent inelastic design spectra: Strength and displacement. *Earthquake Engineering & Structural Dynamics*, 23(5):507–521, may 1994. ISSN 00988847. doi: 10.1002/eqe.4290230504. URL `http://doi.wiley.com/10.1002/eqe.4290230504`.

[46] Eduardo Miranda. Inelastic Displacement Ratios for Structures on Firm Sites. *Journal of Structural Engineering*, 126(10):1150–1159, oct 2000. ISSN 0733-9445. doi: 10.1061/(ASCE)0733-9445(2000)126:10(1150). URL `https://ascelibrary.org/doi/10.1061/{%}28ASCE{%}290733-9445{%}282000{%}29126{%}3A10{%}281150{%}29`.

[47] Athanasia K. Kazantzi and Dimitrios Vamvatsikos. Intensity measure selection for vulnerability studies of building classes. *Earthquake Engineering & Structural Dynamics*, 44(15):2677–2694, dec 2015. ISSN 00988847. doi: 10.1002/eqe.2603. URL `http://doi.wiley.com/10.1002/eqe.2603`.

[48] Mohsen Kohrangi, Paolo Bazzurro, and Dimitrios Vamvatsikos. Vector and Scalar IMs in Structural Response Estimation: Part II – Building Demand Assessment. *Earthquake Spectra*, 32(3):1525–1543, feb 2016. doi: 10.1193/053115EQS081M.

[49] Laura Eads, Eduardo Miranda, and Dimitrios G. Lignos. Average spectral acceleration as an intensity measure for collapse risk assessment. *Earthquake Engineering & Structural*

Dynamics, 44(12):2057–2073, sep 2015. ISSN 00988847. doi: 10.1002/eqe.2575. URL http://doi.wiley.com/10.1002/eqe.2575.

[50] Gerard J. O'Reilly. Limitations of Sa(T1) as an intensity measure when assessing non-ductile infilled RC frame structures. *Bulletin of Earthquake Engineering*, 19(6): 2389–2417, apr 2021. ISSN 1570-761X. doi: 10.1007/s10518-021-01071-7. URL http://link.springer.com/10.1007/s10518-021-01071-7https://link.springer.com/10.1007/s10518-021-01071-7.

[51] FEMA P-58. FEMA P-58-1: Seismic Performance Assessment of Buildings: Volume 1 - Methodology. Technical Report September, Federal Emergency Management Agency, Washington, DC, 2012.

[52] T. J. Sullivan, P. M. Calvi, and R. Nascimbene. Towards improved floor spectra estimates for seismic design. *Earthquakes and Structures*, 4(1):109–132, 2013.

[53] David P. Welch and Timothy John Sullivan. Illustrating a new possibility for the estimation of floor spectra in nonlinear multi-degree of freedom systems. In *16th World Conference on Earthquake Engineering*, Santiago, Chile, 2017.

[54] Roberto J. Merino, Daniele Perrone, and Andre Filiatrault. Consistent floor response spectra for performance-based seismic design of nonstructural elements. *Earthquake Engineering & Structural Dynamics*, 49(3):261–284, mar 2020. ISSN 0098-8847. doi: 10.1002/eqe.3236. URL https://onlinelibrary.wiley.com/doi/abs/10.1002/eqe.3236.

[55] Edmond V. Muho, Chao Pian, Jiangu Qian, Mahdi Shadabfar, and Dimitri E. Beskos. Deformation-dependent peak floor acceleration for the performance-based design of non-structural elements attached to r/c structures. *Earthquake Spectra*, 37:1035 – 1055, 2021. URL https://api.semanticscholar.org/CorpusID:233364871.

[56] Jose Poveda and Gerard J. O'Reilly. Seismic Loss Assessment of Existing Hotel in Ecuador. In *18th World Conference on Earthquake Engineering*, Milan, Italy, 2024.

[57] Omid Esmaili, Lisa Grant Ludwig, and Farzin Zareian. An Applied Method for General Regional Seismic Loss Assessment—With A Case Study in Los Angeles County. *Journal of Earthquake Engineering*, 22(9):1569–1589, oct 2018. ISSN 1363-2469. doi: 10.1080/13632469.2017.1284699. URL https://www.tandfonline.com/doi/full/10.1080/13632469.2017.1284699.

[58] Davit Shahnazaryan, Gerard J. O'Reilly, and Ricardo Monteiro. Story loss functions for seismic design and assessment: Development of tools and application. *Earthquake Spectra*, 37:2813 – 2839, 2021. URL https://api.semanticscholar.org/CorpusID:237774879.

[59] Al Mouayed Bellah Nafeh and Gerard J. O'Reilly. Simplified pushover-based seismic loss assessment for existing infilled frame structures. *Bulletin of Earthquake Engineering*, oct 2023. ISSN 1570-761X. doi: 10.1007/s10518-023-01792-x. URL https://link.springer.com/10.1007/s10518-023-01792-x.

[60] Gerard J. O'Reilly, Al Mouayed Bellah Nafeh, and Davit Shahnazaryan. Simplified tools for the risk assessment and classification of existing buildings. *Procedia Structural Integrity*, 44:1744–1751, 2023. ISSN 24523216. doi: 10.1016/j.prostr.2023.01.223. URL https://linkinghub.elsevier.com/retrieve/pii/S2452321623002329.

[61] C. M. Ramirez and E. Miranda. Significance of residual drifts in building earthquake loss estimation. *Earthquake Engineering & Structural Dynamics*, 41(11):1477–1493, sep 2012. ISSN 00988847. doi: 10.1002/eqe.2217. URL http://doi.wiley.com/10.1002/eqe.2217.

[62] Jenna Jihyun Kim, Kenneth J. Elwood, Frederic Marquis, and Stephanie E. Chang. Factors Influencing Post-Earthquake Decisions on Buildings in Christchurch, New Zealand. *Earthquake Spectra*, 33(2):623–640, 2017. ISSN 8755-2930. doi: 10.1193/072516EQS120M. URL http://earthquakespectra.org/doi/10.1193/072516EQS120M.

[63] Minjie Zhu, Frank McKenna, and Michael H. Scott. Openseespy: Python library for the opensees finite element framework. *SoftwareX*, 7:6–11, 2018. URL https://api.semanticscholar.org/CorpusID:64780757.

[64] F. Jalayer and C. A. Cornell. Alternative non-linear demand estimation methods for probability-based seismic assessments. *Earthquake Engineering & Structural Dynamics*, 38(8):951–972, jul 2009. ISSN 00988847. doi: 10.1002/eqe.876. URL http://doi.wiley.com/10.1002/eqe.876.

[65] Timothy D. Ancheta, Robert B. Darragh, Jonathan P. Stewart, Emel Seyhan, Walter J. Silva, Brian S.-J. Chiou, Katie E. Wooddell, Robert W. Graves, Albert R. Kottke, David M. Boore, Tadahiro Kishida, and Jennifer L. Donahue. Nga-west2 database. *Earthquake Spectra*, 30:1005 – 989, 2014. URL https://api.semanticscholar.org/CorpusID:55149911.